ARTICLE IN PRESS

Extreme Mechanics Letters ▮ (▮▮▮▮) ▮▮▮–▮▮▮

Contents lists available at ScienceDirect

Extreme Mechanics Letters

journal homepage: www.elsevier.com/locate/eml

Failure mechanics of a wrinkling thin film anode on a substrate under cyclic charging and discharging

Zheng Jia, Teng Li *

Department of Mechanical Engineering, University of Maryland, College Park, MD 20742, USA

GRAPHICAL ABSTRACT

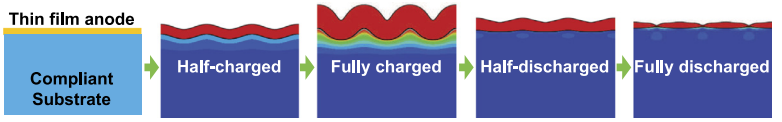

ARTICLE INFO

Article history:
Received 1 January 2016
Received in revised form 7 March 2016
Accepted 8 March 2016
Available online xxxx

Keywords:
Anode
Wrinkling
Necking
Thin film

ABSTRACT

Recent experiments show that a thin film anode on a compliant substrate can significantly mitigate mechanical degradation and capacity fading of lithium-ion and sodium-ion batteries in service. The enhanced cycle performance of such a substrate-supported thin film anode is attributed to the wrinkling-induced stress relaxation. While the experimental evidence is suggestive, there lacks a systematic mechanistic study of the wrinkling of the substrate-supported thin film anode and its influence on anode cycle performance. We report a comprehensive study of the charging/discharging induced wrinkling formation and subsequent morphologic evolution of a substrate-supported thin film anode, using theoretical analysis and finite element simulations. We reveal that necking bands may form near wrinkling troughs or peaks and further develop to cause fragmentation of the anode over charging/discharging cycles, a failure mode not reported in the existing literature. The density and distribution of the wrinkling-associated necking bands in the substrate-supported thin film anode can be regulated by the substrate stiffness. Moreover, the wrinkling-induced necking in such a thin film anode can be deferred by regulating the charging capacity. These findings offer new mechanistic understanding of substrate-supported thin film anodes and thus shed light on novel design of high performance anodes in batteries.

1. Introduction

The past decade has seen a surge of interest in developing next-generation rechargeable batteries with high capacity and long cycling life with an array of diverse applications ranging from portable electronics to electric vehicles, and to grid scale energy storage [1–7]. There exist intensive studies to search candidate electrodes with high electrochemical capacity and mechanical durability. For example, silicon (Si) has the highest theoretical capacity of 4200 mAh/g when fully lithiated in lithium-ion (Li-ion) batteries [8] and tin (Sn) alloys with sodium (Na) in Na-ion batteries at a capacity of 847 mAh/g when $Na_{15}Sn_4$

* Corresponding author.
E-mail address: lit@umd.edu (T. Li).

http://dx.doi.org/10.1016/j.eml.2016.03.006
2352-4316/

Please cite this article in press as: Z. Jia, T. Li, Failure mechanics of a wrinkling thin film anode on a substrate under cyclic charging and discharging, Extreme Mechanics Letters (2016), http://dx.doi.org/10.1016/j.eml.2016.03.006

is formed [9]. However, extreme volumetric expansion (e.g., 300%–400%) is often associated with the fully charged state of such electrode materials, which in turn causes anode pulverization and thus leads to rapid capacity fading and poor cycle performance of the batteries [10–15]. Therefore, averting the mechanical degradation of anodes induced by the extreme volumetric change during charging/discharging cycles remains as one of the major challenges in developing high performance Li-ion and Na-ion batteries.

Tremendous efforts have been focused on mitigating the mechanical failure of anodes in high-performance Li-ion and Na-ion batteries. Charging/discharging-induced stress and associated mechanical failure in Si and Sn anodes are widely studied through experimental characterization [16–19] and chemo-mechanical modeling [11,13,20–30]. As revealed from these studies, size reduction, geometry optimization and surface passivation of the anodes are shown to be able to mitigate excessive stresses induced during charging/discharging and thus help avoid pulverization of anodes [12,13,20,31]. For example, it has been demonstrated that nanoscale Si anodes, such as nanowires [32], nano-particles, nano-beads [31], nano-walls [33] and nano-sized thin films [34] exhibit superior cycle performance than their bulk counterparts [35], largely due to the reduced driving force for crack propagation in such anodes. Hollow Si nanowires and nanospheres are shown to not only relieve lithiation-induced stresses but also reduce the impeding effect of such stresses on lithiation kinetics [36]. Surface passivation of anodes using functional coatings such as carbon [37], nickel [38,39], silicon oxides [40,41] and aluminum oxides [9] can avoid the repeated formation of excess solid-electrolyte-interface (SEI) layers and mediate mechanical degradation of anodes such as fracture and detachment from current collector [42].

It has been shown that a thin film can be made deformable by leveraging out-of-the-plane buckling and wrinkling to accommodate large in-plane deformation without resulting in significant strain in the film material [43,44]. Such a concept has been successfully used in designing highly deformable flexible electronic devices [45–47], and recently been applied to design durable anode structures that can sustain the huge deformation associated with charging/discharging. For example, Bhandakkar et al. computationally demonstrate that honeycomb-shaped anodes allow for buckling deformation mode during lithiation and delithiation, which effectively reduces the resulting stresses [48]. Yu et al. reported that Polydimethylsiloxane (PDMS)-supported thin ribbon Si anodes can yield a cycle performance up to 500 cycles with nearly 85% capacity retention [34], which is attributed to the mitigation of lithiation-induced stresses via wrinkling of the Si ribbons. Zhu et al. showed that an anode for Na-ion battery consisting of a thin Sn film bonded to a soft wood fiber substrate can sustain more than 400 charging/discharging cycles, while a similar thin film Sn anode on a rigid substrate suffers from severe capacity decay after only 10 s cycles [9]. Chemomechanical modeling reveals that the wrinkling of the Sn film during sodiation/desodiation leads to effective stress relaxation, a key to the enhanced mechanical integrity and electrochemical performance of the anode.

While the experimental evidence of leveraging wrinkling for designing durable anodes is suggestive, there lacks a systematic mechanistic study of the wrinkling of substrate-supported thin film anodes and its influence on anode cycle performance. Some fundamental but crucial questions remain elusive so far. For instance, while it is shown that wrinkling can lead to stress relaxation in thin film anodes, it remains unclear what is the fundamental deformation mechanism that governs the mechanical failure of such wrinkling thin film anodes under cyclic charging/discharging. Furthermore, existing computational studies of the wrinkling thin film anodes are conducted for only the first charging/discharging cycle. How does the wrinkling morphology of the thin film anode evolve over cycles and how does such an evolution of wrinkling morphology subsequently affect the battery performance? Aiming to address these open questions, in this paper, we report a comprehensive study of the charging/discharging induced wrinkling formation and subsequent morphologic evolution of a substrate-supported thin film anode, using both theoretical analysis and finite element simulations.

Emerging from the present comprehensive study is a failure mechanism of a thin film anode supported by a compliant substrate subject to electrochemical charging/discharging cycles that is distinct from that of a thin film anode supported by a stiff substrate. Fig. 1 summarizes the difference in the failure mechanisms of these two anode architectures. During the first charging half cycle, the thin film anode thickens to accommodate the volume increase due to ion insertion. The substrate constraint further increases the compressive stress in the thin film anode. Well bonded to a stiff substrate, the thin film anode remains planar during the charging half cycle. By contrast, on a compliant substrate, the thin film anode starts to wrinkle, driven by the charging-induced compressive stress and accommodated by the substrate distortion. As to be shown later, the wrinkling occurs in a rather periodic manner with a wavelength λ_w that is governed by the anode thickness and the anode/substrate stiffness ratio. During the first discharging half cycle, ion extraction causes the thinning of the anode. Consequently, on a stiff substrate, substantial tensile stress builds up in the thin film anode so that channel cracks may initiate and propagate in the anode in a rather random fashion. By contrast, during the first discharging half cycle, the wrinkled thin film anode on a compliant substrate thins and flattens simultaneously, accompanied by a peculiar feature of necking formation in the thin film anode near the troughs or peaks of the wrinkling morphology. In subsequent charging/discharging cycles, the above morphological evolution of the thin film anode continues, leading to two distinct mechanical failure modes of the two anode architectures. For a thin film anode bonded to a stiff substrate, more and more channel cracks form and propagate in the anode in a random fashion, eventually causing the pulverization of the anode, as observed in many experiments [49,50]. By contrast, for a thin film anode bonded to a compliant substrate, the wrinkling

Please cite this article in press as: Z. Jia, T. Li, Failure mechanics of a wrinkling thin film anode on a substrate under cyclic charging and discharging, Extreme Mechanics Letters (2016), http://dx.doi.org/10.1016/j.eml.2016.03.006

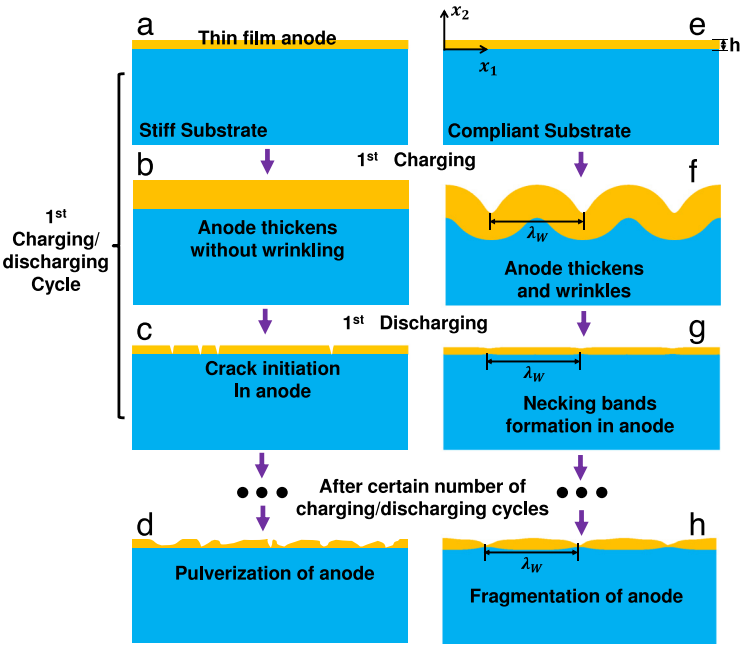

Fig. 1. Schematic of morphological evolution and associated failure of a substrate-supported thin film anode during electrochemical cycles: (a–d) a thin film anode bonded to a stiff substrate; (e–h) a thin film anode bonded to a compliant substrate. On a stiff substrate, during the 1st charging half cycle (b), the anode first thickens to accommodate the volume expansion. No wrinkling occurs in the thin film anode due to the substrate constraint. In the subsequent 1st discharging half cycle (c), the anode thins down, and meanwhile random channel cracks start to initiate and propagate in the thin film anode under substantial tensile stress. Anode film pulverizes over cycles due to repeated formation of random cracks (d). On a compliant substrate, during the 1st charging half cycle (f), the thin film anode starts to wrinkle with a wavelength of λ_w driven by the charging-induced compressive stress and accommodated by the substrate distortion. In the 1st discharging half cycle (g), the necking forms at the wrinkling troughs/peaks due to discharging-induced tension. (h) Over cycling, periodic cracks form at the sites of necking bands, leading to the fragmentation of the anode.

morphology is set by the first charging/discharging cycle, and the anode eventually fails by fragmentation due to the progressive development of the necks bands near the troughs and peaks of the wrinkling morphology. This failure mechanism of compliant-substrate-supported thin film anodes is not reported in the existing literature, and offers new mechanistic understanding of substrate-supported thin film anodes and thus shed light on novel design of high performance anodes in Li-ion and Na-ion batteries. We next delineate a comprehensive study on this new failure mechanism in details and elaborate the potential insights on optimal anode design derived from this mechanistic finding.

2. Initiation of wrinkling of a thin film anode supported by a compliant substrate

We first present a theoretical formulation to quantify the wrinkling and yielding behavior of an elastoplastic thin film anode supported by a compliant hyperelastic substrate. The Young's modulus, Poisson's ratio and yielding stress of the anode material are denoted by E_f, ν and σ_Y, respectively. The hyperelastic substrate is taken as a neo-Hookean material with a shear modulus at small deformation denoted by μ_s. The thickness of the pristine thin film anode is h. The anode is in the plane of (x_1, x_3) with a surface normal along x_2 direction. The hyperelastic substrate is assumed to be infinitely thick, which is justified by the huge anode/substrate thickness ratio in real anode architectures (e.g., >1000). In this work, we study substrate-supported thin-film anodes operating at normal charging rates (e.g., C/10) used in typical battery testing. Such a charging rate is much slower than the Li (or Na) ion diffusion and reaction in the anode. So it is reasonable to assume a uniform charging-induced volume expansion of the anode. For the anode/substrate bilayer shown in Fig. 1(a) (or Fig. 1(e)), the charging-induced uniform volume expansion of the anode is constrained by the underlying substrate. Therefore, the unwrinkled thin film anode is in a uniform in-plane stress state given by $\sigma_{11} = \sigma_{33} = -\sigma$. Assuming the thin film anode remains elastic before wrinkling occurs, the out-of-plane deflection of the anode is governed by the von Karman plate equation [51]

$$D\nabla^4 w + \sigma h \nabla^2 w = -T \tag{1}$$

where ∇^4 is the bi-harmonic operator, $D = E_f h^3/[12(1-\nu^2)]$ denotes the bending stiffness of the thin film anode, w is the out-of-plane deflection displacement in x_2 direction, and T is the stress component acting perpendicular to the anode that is exerted by the substrate. Considering a one dimensional wrinkling pattern in the (x_1, x_2) plane, the above governing equation admits solutions in the form of $w = \hat{w}\cos(kx_1)$ and $T = \hat{T}\cos(kx_1)$, which gives

$$\left(Dk^4 - \sigma h k^2\right)\hat{w} = -\hat{T}, \tag{2}$$

with k being the wave number of the wrinkling. Solving a Boussinesq problem for a semi-infinite neo-Hookean

Please cite this article in press as: Z. Jia, T. Li, Failure mechanics of a wrinkling thin film anode on a substrate under cyclic charging and discharging, Extreme Mechanics Letters (2016), http://dx.doi.org/10.1016/j.eml.2016.03.006

substrate gives [52]

$$\hat{T} = 2\mu_s k\hat{w}. \tag{3}$$

Combining Eqs. (2) and (3) yields an eigenvalue equation $\sigma = \frac{D}{t}k^2 + 2\frac{\mu_s}{t}\frac{1}{k}$. The minimum eigenvalue σ_c defines the critical wrinkling stress, which is obtained at $k_c = \left(\frac{\mu_s}{D}\right)^{\frac{1}{3}}$ and given by

$$\sigma_c = \bar{E}_f \left(\frac{3}{2}\frac{\mu_s}{\bar{E}_f}\right)^{\frac{2}{3}} \tag{4}$$

with $\bar{E}_f = E_f/(1-\nu^2)$. The corresponding wrinkling wavelength (defined in Fig. 1(f)) can be computed by

$$\lambda_w = \frac{2\pi}{k_c} = 2\pi h \left(\frac{\bar{E}_f}{12\mu_s}\right)^{\frac{1}{3}}. \tag{5}$$

The above theoretical analysis holds for the case that the thin film anode remains elastic before wrinkling occurs. As to be shown by finite element simulations in Section 3, for the anode/substrate bilayer in Fig. 1(a) and (e), if the critical wrinkling stress σ_c defined by Eq. (4) is lower than σ_Y (note that the yielding stress of an elastoplastic film under equi-biaxial compression equals the yield strength σ_Y of the film material), the thin film anode wrinkles elastically prior to yielding and the corresponding wrinkling occurs at a wavelength in excellent agreement with the prediction by Eq. (5). However, if the critical wrinkling stress σ_c is higher than σ_Y, the thin film anode first yields, followed by plastic wrinkling with a wavelength that slightly deviates from that predicted by Eq. (5), as to be detailed in Section 3.

The above competing interplay between wrinkling and yielding can be captured by a dimensionless parameter Λ as the ratio between the critical wrinkling stress σ_c and yielding stress of the anode material σ_Y, that is

$$\Lambda = \frac{\sigma_c}{\sigma_Y} = \frac{\bar{E}_f}{\sigma_Y}\left(\frac{3}{2}\frac{\mu_s}{\bar{E}_f}\right)^{\frac{2}{3}}. \tag{6}$$

The physical significance of Λ is as follows. If $\Lambda < 1$, elastic wrinkling occurs prior to yielding of the anode; upon the onset of elastic wrinkling, stresses in the thin film anode are partially relaxed; upon further charging, stresses may build up in the anode and cause yielding. If $\Lambda \geq 1$, the anode yields before wrinkling occurs; with further volume expansion due to charging, the anode wrinkles plastically. It is worth noting that, the value of Λ reflects the interplay between material properties of the thin film anode and the substrate. For example, for a given anode material, the value of Λ can be tuned by changing the substrate material (e.g., a stiffer substrate leads to a greater value of Λ). As to be further shown in Section 4, the dimensionless parameter Λ not only describes the competing interplay between wrinkling and yielding, but also characterizes the failure modes of the thin film anodes under cyclic charging/discharging. The theoretical analysis in this section will be used to benchmark the finite element modeling results in Section 3 and provide insights into the anode failure modes in Section 4.

3. Evolution of wrinkling morphology of substrate-supported thin film anodes

The theoretical formulation in Section 2 holds for the case of elastic wrinkling prior to yielding (i.e., $\Lambda < 1$), and is based on an eigenvalue analysis, so that does not account for post-wrinkling. In this section, we carry out comprehensive finite element simulations to investigate the charging/discharging induced deformation behaviors of a substrate-supported thin film anode, from incipient wrinkling to large amplitude post-wrinkling and for the full range of values of Λ.

In finite element simulations, the thin film anode material is taken to be an elastic and perfectly plastic materials with $E_f = 30$ GPa, $\nu = 0.3$ and $\sigma_Y = 2$ GPa, which are representative for Si (or Sn) anodes in Li-ion (or Na-ion) batteries [22,33,53,54]. The substrate is considered as a neo-Hookean material with an initial shear modulus μ_s. To study the effect of the substrate stiffness on the wrinkling of the thin film anode, μ_s is varied from 100 MPa to 2.5 GPa, which corresponds to the range of Λ from 0.22 to 1.86. The simulations are carried out using ABAQUS Explicit package. Charging-induced volume change of the anode material is introduced to the thin film anode through a thermal strain analogy, with the full charge corresponding to 300% volume expansion [22,31]. The state of charge (SOC) is defined as the ratio between the current ion concentration in the anode over the ion concentration at fully charged state (e.g., SOC = 0 being the pristine state and SOC = 1 fully charged state). As charging proceeds, compressive in-plane stress develops in the thin film anode due to the constraint from the underlying substrate. Wrinkling initiates once the compressive in-plane stress exceeds the critical stress defined by Eq. (4), and further evolves as SOC increases. Fig. 2 presents the morphology of the substrate-supported thin film anode at SOC = 0.5 and SOC = 1 during the first charging half cycle for various values of Λ. On a sufficiently stiff substrate (e.g., $E_s = 2.5$ GPa, $\Lambda = 1.86$), the out-of-the-plane deformation of the thin film anode is fully constrained, so that the anode remains flat without wrinkling and only thickens due to ion insertion during charging (Fig. 2(a) and (b)). With $\Lambda = 1.60$ (i.e., $E_s = 2$ GPa), under charging the thin film anode first fully yields prior to the onset of wrinkling. As the SOC increases, wrinkling and thickening of the thin film anode develop simultaneously (Fig. 2(c)). As a result, a sharp V-shaped morphology forms at the top surface of wrinkling troughs, which can be explained in twofold: (i) half of the wrinkling wavelength in this case ($\sim 5.4h$) is comparable to the final film thickness of the fully charged anode ($\sim 4h$). Therefore, large amplitude wrinkling leads to finite shear stress, which may cause severe local distortion in segments of the thin film anode (as highlighted by the dashed box in Fig. 2(d)); (ii) the substrate is relatively stiff so that the deformation of the anode near the anode/substrate is more confined than the anode portion near its free top surface. As a result, fold-like V-shaped sharp features occur at the top surface of wrinkling troughs while the anode/substrate interface near wrinkling peaks distorts modestly. The significance of such a deformation characteristic during

Please cite this article in press as: Z. Jia, T. Li, Failure mechanics of a wrinkling thin film anode on a substrate under cyclic charging and discharging, Extreme Mechanics Letters (2016), http://dx.doi.org/10.1016/j.eml.2016.03.006

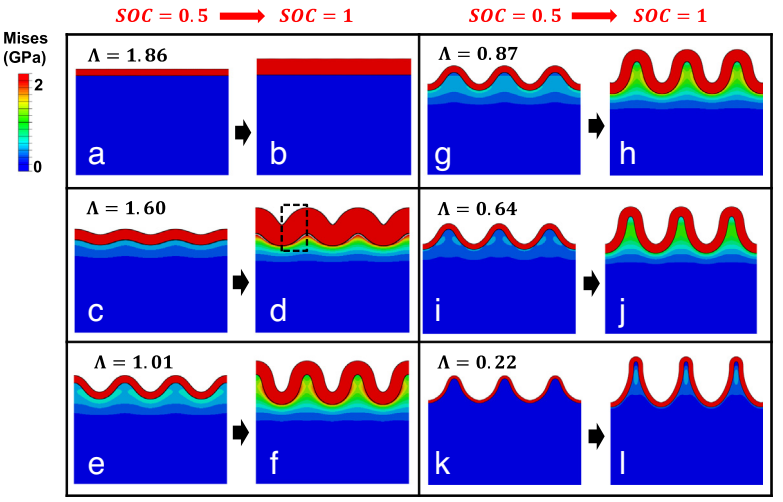

Fig. 2. Finite element simulation results on wrinkling morphology evolution of substrate-supported thin-film anodes at SOC = 0.5 and SOC = 1 in the 1st charging half cycle, for various values of Λ. (a,b) $\Lambda = 1.86$, the thin film anode only thickens without wrinkling due to the substrate constraint; (c,d) $\Lambda = 1.6$, wrinkling morphology develops and sharp V-shaped features form at the top surface of wrinkling troughs. (e–j) $\Lambda = 1.01$, 0.87 and 0.64, respectively, wrinkling forms during charging with a sinusoidal shape. (k–l) $\Lambda = 0.22$, wrinkling forms with sharp peaks accommodated by the severe distortion of the compliant substrate. Color contour denotes the von-Mises stress level. (For interpretation of the references to color in this figure legend, the reader is referred to the web version of this article.)

charging on the mechanical failure mechanism of the anode will be discussed in Section 4. A compliant substrate yields a smaller Λ, and thus a longer wrinkling wavelength as well as a larger wrinkling amplitude for a given SOC (e.g., Fig. 2(e)–(j)). In such cases, the wrinkled morphology of the thin film anode is rather smooth, without acute folds at wrinkling peaks or troughs. On a very compliant substrate (e.g., $E_s = 0.1$ GPa, $\Lambda = 0.22$, Fig. 2(k) and (l)), wrinkling occurs in the thin film anode before yielding, at a wavelength much larger than the anode thickness, and develops into large amplitude as charging proceeds. At fully charged state (SOC = 1), large amplitude wrinkling of the thin film anode causes severe distortion of the compliant substrate near the interface at wrinkling peaks.

To further quantify the wrinkling morphology, Fig. 3 plots the wrinkling wavelength λ_w (triangle markers) and amplitude A (square markers) at fully charged state (SOC = 1) as a function of Λ. Both λ_w and A decrease when the underlying substrate becomes stiffer (i.e., increasing Λ). There exists a critical value of substrate stiffness, above which thin film anode only thickens without wrinkling during charging. Lack of wrinkling-facilitated stress relaxation, randomly distributed cracks can initiate and propagate in the thin film anode over charging/discharging cycles, which eventually pulverize the anode and causing irreversible capacity fading [35], as illustrated in Fig. 1(a)–(d). Our simulations suggest that such a critical substrate stiffness ranges between 2 GPa and 2.5 GPa, corresponding to a critical value of Λ_c between 1.60 and 1.86. If $1 \leq \Lambda < \Lambda_c$, the thin film anode yields prior to the onset of plastic wrinkling; while if $\Lambda < 1$, elastic wrinkling occurs in the thin film anode first before yielding, which sets in later upon wrinkling deformation developing significantly. The wrinkling wavelength emerging from finite element simulations is shown to be in excellent agreement with the theoretical prediction by Eq. (5) when $\Lambda < 1$, and is slightly greater than the theoretical prediction when $1 \leq \Lambda < \Lambda_c$. Fig. 3 offers quantitative guidelines on material selection in the anode-on-substrate architecture in battery design to leverage wrinkling-facilitated stress relaxation during charging/discharging for a better cycle performance.

4. Wrinkling-associated deformation and failure mechanisms of substrate-supported thin film anodes in subsequent charging/discharging cycles

The study in Sections 2 and 3 focuses on the first charging half cycle. To further understand the influence of wrinkling on the structural integrity and performance of the thin film anodes over cycles, in this section, we will study how the wrinkling morphology evolves over charging/discharging cycles and how the evolution of wrinkling morphology affects mechanical deformation and failure of such anodes.

After the first charging half cycle, extraction of ions from the anode in the subsequent discharging half cycle causes contraction of the anode, which is first accommodated by flattening of the wrinkling deformation as well as thinning of the anode. Further contraction of the anode is constrained by the underlying substrate. As a result, tensile stress builds up and accumulates in the plane of the thin film anode during discharging. Fig. 4 shows the snapshots of the deformation evolution of the thin film anode, from the wrinkled morphology at fully charged state SOC = 1, to a partially discharged state (SOC = 0.5) and the fully discharged state (SOC = 0), in the first discharging half cycle. On a stiff substrate (e.g., $E_s = 2$ GPa, $\Lambda = 1.60$), the wrinkled anode flattens and thins significantly upon discharging from SOC = 1 to SOC = 0.5 (Fig. 4(a)). At SOC = 0.5, the thin film anode shows a nearly flattened bottom surface

Please cite this article in press as: Z. Jia, T. Li, Failure mechanics of a wrinkling thin film anode on a substrate under cyclic charging and discharging, Extreme Mechanics Letters (2016), http://dx.doi.org/10.1016/j.eml.2016.03.006

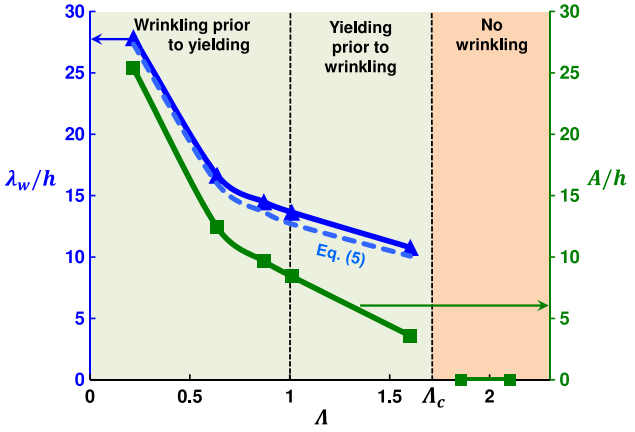

Fig. 3. Finite element simulation results on wrinkling wavelength λ_w (triangle markers) and amplitude A (square markers) of the thin film anode at the first fully charged state as a function of Λ. There exists a critical value Λ_c, above which the substrate-supported thin film anode does not wrinkle under charging. The theoretical prediction of the wrinkling wavelength by Eq. (5) is also included for comparison (dashed line), which shows excellent agreement with finite element simulation results when $\Lambda < 1$, and slightly underestimates if yielding occurs prior to wrinkling ($1 \leq \Lambda < \Lambda_c$).

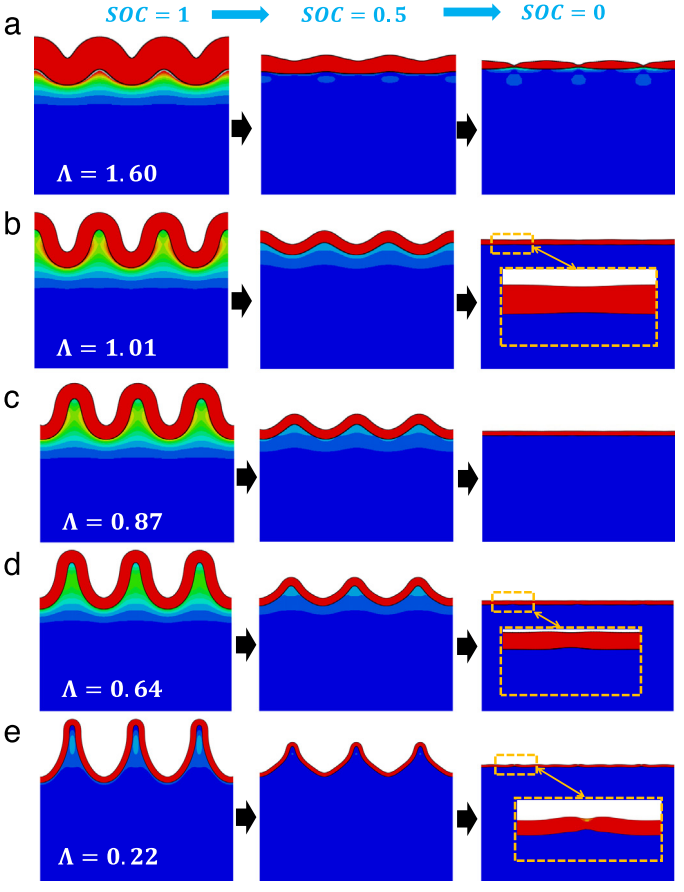

Fig. 4. Morphological evolution of the wrinkled thin film anode during the first discharging half cycle for various values of Λ. Snapshots at fully charged, half discharged, and fully discharged states are shown. As discharging proceeds, wrinkling flattens and the anode thins. Tensile stress builds up in the anode due to substrate constraint, which may cause necking formation at wrinkling troughs (a–b) or wrinkling peaks (d–e).

but a fluctuating top surface, leading to a shape with a non-uniform thickness that is distinct from the sinusoidal shape of the anode with nearly uniform thickness at the same SOC in the first charging half cycle, as shown in Fig. 2(c). The locations of the thinner segments in the half-discharged thin film anode coincide with those of the sharp V-shaped wrinkling troughs (Fig. 2(d)), which can be attributed to shape-retaining due to irreversible plastic

Please cite this article in press as: Z. Jia, T. Li, Failure mechanics of a wrinkling thin film anode on a substrate under cyclic charging and discharging, Extreme Mechanics Letters (2016), http://dx.doi.org/10.1016/j.eml.2016.03.006

deformation. Upon further discharging, tensile stress in the thin film anode increases. The fluctuating thickness of the anode acts as geometric imperfection, causing stress concentration and strain localization (e.g., necking) in the anode under tension at the proximity of the *a priori* wrinkling troughs. At the first fully discharged state (SOC $=$ 0), the necking bands eventually develop into diffusive cracks and cause fragmentation of the thin film anode (Fig. 4(a), right panel). Such a wrinkling-initiated multiple neck formation in a substrate-supported thin film anode under cyclic charging/discharging is distinct from the multiple neck formation in a substrate-supported thin metal film under a uniaxial tension [55–57]. On a less stiff substrate (e.g., $E_s = 1$ GPa, $\Lambda = 1.01$), the discharging half cycle features decreasing wrinkling amplitude and nearly uniform thinning of the thin film anode. By the end of first full discharge, diffusive necking bands of rather modest amplitudes form at the proximity of the *a priori* wrinkling troughs but no fragmentation occurs in the thin film anode (Fig. 4(b), right panel). On a compliant substrate (e.g., $E_s = 0.8$ GPa, $\Lambda = 0.87$), the thin film anode can almost recover its initial flat morphology after the first full discharging without forming any appreciable necking (Fig. 4(c)). On a more compliant substrate (e.g., $E_s = 0.5$ GPa, $\Lambda = 0.64$ (Fig. 4(d)) or $E_s = 0.1$ GPa, $\Lambda = 0.22$ (Fig. 4(e))), after the first full discharging, the thin film anode can resume a flat morphology but necking bands set in at the proximity of the *a priori* wrinkling peaks. The more compliant the substrate, the larger the necking amplitude in the anode at the first full discharged state. This can be explained by the fact that the severe plastic deformation of the thin film anode near its bottom surface at the sharp wrinkling peaks at the end of first full charge (Fig. 2(l)) acts as geometric imperfection to initiate necking formation during discharging. Results in Fig. 4 shed new insights on the dual role of wrinkling deformation on the mechanical integrity of substrate-supported thin film anodes: on one hand, wrinkling can effectively mitigate the severe deformation and thus the resulting stress associated with charging [9,34,48]; on the other hand, it may induce mechanical degradation of the thin film anode by facilitating the formation of necking band during the first discharging half cycle.

We further study the morphological evolution of the substrate-supported thin film anode in the second charging/discharging cycle. Results of three representative cases, with $\Lambda = 1.01$, 0.87 and 0.22, respectively, are shown in Fig. 5. In all three cases, wrinkle re-appears at exactly the same locations in the thin film anode to accommodate the associated volume expansion upon second charging; and the wrinkled morphology of the anode flattens upon second discharging. For the case of $\Lambda = 1.01$ (Fig. 5(a)), at the second fully charged state, sharp V-shaped morphology forms at the top surface of wrinkling troughs, in contrast with the smooth sinusoidal shape of the top surface at the first fully charged state. Upon the subsequent second discharging, such sharp V-shaped features serve as geometric imperfections and causes necking band formation at the wrinkling troughs, which eventually leads to the fragmentation of the thin film anode at the second fully discharged state. For the case of $\Lambda = 0.87$ (Fig. 5(b)), even though no appreciable necking occurs at the end of the first charging/discharging cycle (Fig. 4(c)), necking bands can form during the second discharging half cycle at the wrinkling troughs. At the second fully discharged state, some necking bands can even further develop into cracks to cause fragmentation of the anode. Such a "deferred" formation of necking bands and cracks can be possibly attributed to the plastic ratcheting of the thin film anode during repeated charging/discharging. For the case of $\Lambda = 0.22$ (Fig. 5(c)), at the second fully charged state, a crease-like sharp feature occurs at the bottom surface of the wrinkling peaks, following the necking formation at the first fully discharged state. Such sharp features evolve into cracks upon the second full discharging, causing the fragmentation of the thin film anode.

The studies above reveal that fragmentation caused by severe necking is the dominant failure mechanism of a wrinkling thin film anode on a substrate under cyclic charging/discharging. The necking formation and development result from the significant deformation associated with ion insertion/extraction during charging/discharging. As the magnitude of anode deformation is intrinsically related to the amount of ions inserted into (or extracted from) the anode, it is expected that the mechanical degradation and thus the cycle performance of the anode should depend on the charging capacity during service cycles. To demonstrate such dependence, we simulate the morphological evolution of a substrate-supported thin film anode under cyclic charging/discharging with a partial charging capacity. Fig. 6 plots the morphology of the substrate-supported thin film anode after 1st, 3rd, 4th and 5th discharging half cycle for 50% charging capacity (i.e., corresponding to 150% volume expansion after charging half cycle) and that after 1st, 3rd, 5th and 10th discharging half cycle for 25% charging capacity. Here $\Lambda = 1.01$. It has been shown in Fig. 4(b) and Fig. 5(a) that, at full charging capacity, necking bands appear after the 1st discharging cycle in such an anode, which further develop into cracks after the 2nd discharging cycle. Fig. 6(a) shows that the crack formation in the anode can be deferred to the end of the 5th discharging cycle if the anode is charged with 50% of its full capacity. Moreover, if the charging is reduced to 25% of its full capacity, the thin film anode remains nearly intact after 10 charging/discharging cycles (further cycles not performed only due to the constraint of computation expense), without appreciable necking band formation (Fig. 6(b)). Results in Fig. 6 suggest that the mechanical degradation of substrate-supported anodes can be deferred or even avoided by compromising the charging capacity of the anodes, another dimension in designing high performance batteries with better cycle life. The model prediction here is well in line with recent experimental observations in which a thin film Sn anode supported by a soft wood fiber in a Na-ion battery can sustain 400 charging/discharging cycles without significant capacity fading if the anode is charged up to 25% of its theoretical full capacity [9].

In our study, the elastic modulus of the anode material is assumed to be a constant during charging/discharging. Recent researches suggest that the elastic modulus of the

Please cite this article in press as: Z. Jia, T. Li, Failure mechanics of a wrinkling thin film anode on a substrate under cyclic charging and discharging, Extreme Mechanics Letters (2016), http://dx.doi.org/10.1016/j.eml.2016.03.006

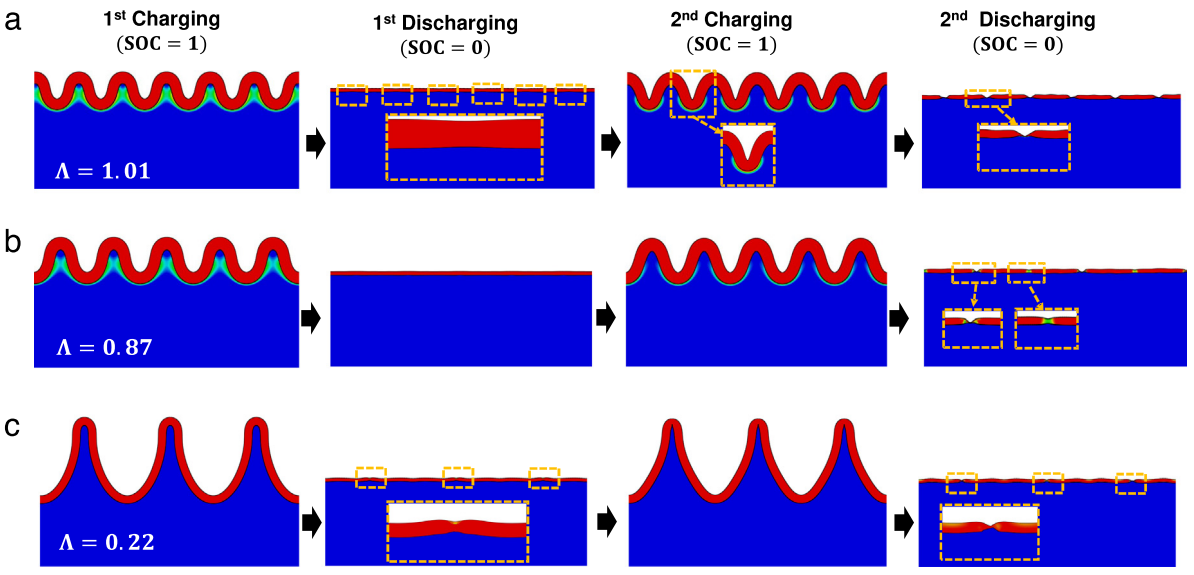

Fig. 5. Morphological evolution of the thin film anode during the first two charging/discharging cycles for various values of Λ. (a) $\Lambda = 1.01$. Following the 1st charging/discharging cycle, sharp V-shaped features form at wrinkling troughs during the 2nd charging half cycle, which further evolve into necking bands during the 2nd discharging, leading to the fragmentation of the anode. (b) $\Lambda = 0.87$. Even though no necking bands form at the end of the 1st discharging, plastic ratcheting leads to necking band formation at wrinkling troughs during the 2nd discharging, and some necking bands further develop into cracks at the end of the 2nd discharging. (c) $\Lambda = 0.22$. Necking band formed at the end of the 1st discharging develops into crease-like sharp feature at the anode/substrate interface during the 2nd charging, which further leads to fragmentation of the anode at the end of the 2nd discharging.

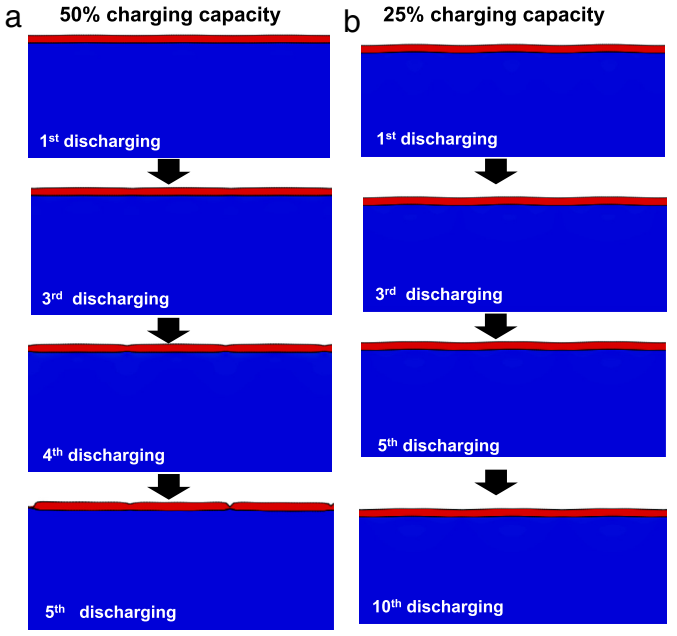

Fig. 6. Morphological evolution of the thin film anode over multiple charging/discharging cycles under (a) 50% charging capacity and (b) 25% charging capacity. Here $\Lambda = 1.01$. Snapshots at the end of each discharging half cycle are shown. At 50% charging capacity, anode fragmentation is deferred to the end of the 5th charging/discharging cycle, while at 25% charging capacity, no appreciable necking bands form at the end of the 10th charging/discharging cycle.

anode decreases under charging [54,58]. It is expected that such elastic softening can help mitigate charging-induced stress in the anode [59]. Above said, the present study may to some extent underestimate the cycle performance of thin film anodes supported by a substrate, but the revealed key deformation characteristics and dominant failure mechanisms of such thin film anodes still hold. Also in this work we assume the perfect bonding between the thin film anode and the substrate. In reality, interfacial defects may exist in the anode/substrate interface during synthesis, or interfacial delamination may initiate under cyclic charging/discharging. Such interfacial

Please cite this article in press as: Z. Jia, T. Li, Failure mechanics of a wrinkling thin film anode on a substrate under cyclic charging and discharging, Extreme Mechanics Letters (2016), http://dx.doi.org/10.1016/j.eml.2016.03.006

defects/delamination are expected to influence the failure mode of the substrate-supported thin films [60], which deserves further systematic study.

5. Concluding remarks

We conduct a theoretical analysis and comprehensive finite element simulations to investigate the evolution of wrinkling morphology of a substrate-supported thin film anode and its influence on the mechanical integrity of the anode under cyclic charging/discharging. For a given anode material, there exists a critical substrate stiffness, above which the thin film anode remains flat during charging/discharging and its mechanical failure mainly results from the initiation and propagation of randomly distributed cracks in the anodes. When supported by a substrate with stiffness lower than the critical value, the thin film anode wrinkles during charging half cycle and flattens during discharging cycle. Our studies reveal the key deformation characteristics and dominant failure mechanisms of such a wrinkling thin film anode on the substrate, distinct from that of a thin film anode on a rigid substrate, as summarized below:

(1) Unlike the randomly distributed cracks formed in a thin film anode on a rigid substrate during charging/discharging, wrinkling of a substrate-supported thin film anode occurs in a periodic manner, with the spacing between neighboring wrinkles (i.e., wrinkling wavelength) proportional to the anode thickness and related to the anode/substrate stiffness ratio (Eq. (5)). The theoretical prediction of the wrinkle spacing agrees well with finite element simulations of the large amplitude deformation of the substrate-supported anode under charging/discharging, and with the experimentally observed wrinkled surface features in a thin film Sn anode supported by a soft wood fiber in a Na-ion battery [9].

(2) The wrinkling-induced plastic deformation in the anode introduces geometric imperfections that further facilitate the formation of necking bands in subsequent charging/discharging cycles. Further development of the necking bands eventually leads to fragmentation, the dominant failure mechanism of the wrinkling thin film anode. The locations of necking bands coincide with the wrinkling peaks and troughs, and interestingly, depends on the substrate stiffness: necking occurs at wrinkling troughs in an anode supported by a stiffer substrate and at wrinkling peaks in an anode supported by a more compliant substrate.

Findings from the comprehensive theoretical analysis and numerical simulations in the present study offer mechanistic understanding of the wrinkling mechanics of a substrate-supported thin film anode during cyclic charging/discharging, from which quantitative guidelines can be drawn to enable optimal design of material combination and service condition toward high performance anodes in advanced batteries.

References

[1] M. Armand, J. Tarascon, Building better batteries, Nature 451 (2008) 652–657.
[2] L. Cui, R. Ruffo, C. Chan, H. Peng, Y. Cui, Crystalline-amorphous core–shell silicon nanowires for high capacity and high current battery electrodes, Nano Lett. 9 (2009) 491–495.
[3] D. Kim, P. Muralidharan, H. Lee, R. Ruffo, Y. Yang, C. Chan, Spinel $LiMn_2O_4$ nanorods as lithium ion battery cathodes, Nano Lett. 8 (2008) 3948–3952.
[4] I. Kovalenko, B. Zdyrko, A. Magasinski, B. Hertzberg, Z. Milicev, R. Burtovyy, A major constituent of brown algae for use in high-capacity Li-ion batteries, Science 334 (2011) 75–79.
[5] R. Marom, S. Amalraj, N. Leifer, D. Jacob, D. Aurbach, A review of advanced and practical lithium battery materials, J. Mater. Chem. 21 (2011) 9938–9954.
[6] R. Van Noorden, A better battery, Nature 507 (2014) 26–28.
[7] R. Service, Tanks for the batteries, Science 344 (2014) 352–354.
[8] B. Boukamp, G. Lesh, R. Huggins, All-solid lithium electrodes with mixed-conductor matrix, J. Electrochem. Soc. 128 (1981) 725–729.
[9] H. Zhu, Z. Jia, Y. Chen, N. Weadock, J. Wan, O. Vaaland, T. Li, L. Hu, Tin anode for sodium-ion batteries using natural wood fiber as a mechanical buffer and electrolyte reservoir, Nano Lett. 13 (2013) 3093–3100.
[10] H. Yang, F. Fan, W. Liang, X. Guo, T. Zhu, S. Zhang, A chemo-mechanical model of lithiation in silicon, J. Mech. Phys. Solids 70 (2014) 349–361.
[11] K. Zhao, M. Pharr, Q. Wan, W.L. Wang, E. Kaxiras, J.J. Vlassak, Z. Suo, Concurrent reaction and plasticity during initial lithiation of crystalline silicon in lithium-ion batteries, J. Electrochem. Soc. 159 (2012) A238–A243.
[12] K. Zhao, M. Pharr, L. Hartle, J. Vlassak, Z. Suo, Fracture and debonding in lithium-ion batteries with electrodes of hollow core–shell nanostructures, J. Power Sources 218 (2012) 6–14.
[13] Y. Hu, X. Zhao, Z. Suo, Averting cracks caused by insertion reaction in lithium-ion batteries, J. Mater. Res. 25 (2010) 1007–1010.
[14] I. Ryu, J. Choi, Y. Cui, W. Nix, Size-dependent fracture of Si nanowire battery anodes, J. Mech. Phys. Solids 59 (2011) 1717–1730.
[15] W. Zhang, A review of the electrochemical performance of alloy anodes for lithium-ion batteries, J. Power Sources 196 (2011) 13–24.
[16] V. Sethuraman, V. Srinivasan, A. Bower, P. Guduru, In Situ measurements of stress-potential coupling in lithiated silicon, J. Electrochem. Soc. 157 (2010) A1253–A1261.
[17] V. Sethuraman, N. Van Winkle, D. Abraham, A. Bower, P. Guduru, Real-time stress measurements in lithium-ion battery negative-electrodes, J. Power Sources 206 (2012) 334–342.
[18] V. Sethuraman, A. Nguyen, M. Chon, S. Nadimpalli, H. Wang, D. Abraham, Stress evolution in composite silicon electrodes during lithiation/delithiation, J. Electrochem. Soc. 160 (2013) A739–A746.
[19] J. Wang, F. Fan, Y. Liu, K. Jungjohann, S. Lee, S. Mao, Structural evolution and pulverization of tin nanoparticles during lithiation-delithiation cycling, J. Electrochem. Soc. 161 (2014) F3019–F3024.
[20] R. Huggins, W. Nix, Decrepitation model for capacity loss during cycling of alloys in rechargeable electrochemical systems, Ionics 6 (2000) 57–63.
[21] S. Huang, F. Fan, J. Li, S. Zhang, T. Zhu, Stress generation during lithiation of high-capacity electrode particles in lithium ion batteries, Acta Mater. 61 (2013) 4354–4364.
[22] H. Yang, S. Huang, X. Huang, F. Fan, W. Liang, X. Liu, S. Zhang, Orientation-dependent interfacial mobility governs the anisotropic swelling in lithiated silicon nanowires, Nano Lett. 12 (2012) 1953–1958.
[23] A. Bower, P. Guduru, V. Sethuraman, A finite strain model of stress, diffusion, plastic flow, and electrochemical reactions in a lithium-ion half-cell, J. Mech. Phys. Solids 59 (2011) 804–828.
[24] J. Christensen, J. Newman, Stress generation and fracture in lithium insertion materials, J. Solid State Electrochem. 10 (2006) 293–319.
[25] Y. Gao, M. Zhou, Coupled mechano-diffusional driving forces for fracture in electrode materials, J. Power Sources 230 (2013) 176–193.
[26] L. Chen, F. Fan, L. Hong, J. Chen, Y. Ji, S. Zhang, A phase-field model coupled with large elasto-plastic deformation: application to lithiated silicon electrodes, J. Electrochem. Soc. 161 (2014) F3164–F3172.
[27] H. Yang, W. Liang, X. Guo, C. Wang, S. Zhang, Strong kinetics-stress coupling in lithiation of Si and Ge anodes, Extreme Mech. Lett. 2 (2015) 1–6.
[28] X. Zhang, S. Lee, H. Lee, Y. Cui, C. Linder, A reaction-controlled diffusion model for the lithiation of silicon in lithium-ion batteries, Extreme Mech. Lett. 4 (2015) 61–75.

Please cite this article in press as: Z. Jia, T. Li, Failure mechanics of a wrinkling thin film anode on a substrate under cyclic charging and discharging, Extreme Mechanics Letters (2016), http://dx.doi.org/10.1016/j.eml.2016.03.006

[29] S. Lee, J. Yang, W. Lu, Debonding at the interface between active particles and PVDF binder in Li-ion batteries, Extreme Mech. Lett. 6 (2016) 37–44.
[30] R. Xu, K. Zhao, Mechanical interactions regulated kinetics and morphology of composite electrodes in Li-ion batteries, Extreme Mech. Lett. (2015).
[31] C. Sun, K. Karki, Z. Jia, H. Liao, Y. Zhang, T. Li, Y. Qi, Y. Wang, A beaded-string silicon anode, ACS Nano 7 (2013) 2717–2724.
[32] K. Karki, E. Epstein, J. Cho, Z. Jia, T. Li, S. Picraux, J. Cummings, Lithium-assisted electrochemical welding in silicon nanowire battery electrodes, Nano Lett. 12 (2012) 1392–1397.
[33] J. Wan, A. Kaplan, J. Zheng, X. Han, Y. Chen, N. Weadock, T. Li, L. Hu, Two dimensional silicon nanowalls for lithium ion batteries, J. Mater. Chem. A 2 (2014) 6051–6057.
[34] C. Yu, X. Li, T. Ma, J. Rong, R. Zhang, J. Shaffer, H. Jiang, Silicon thin films as anodes for high-performance lithium-ion batteries with effective stress relaxation, Adv. Energy Mater. 2 (2012) 68–73.
[35] C. Chan, H. Peng, G. Liu, K. McIlwrath, X. Zhang, R. Huggins, Y. Cui, High-performance lithium battery anodes using silicon nanowires, Nature Nanotechnol. 3 (2008) 31–35.
[36] Y. Yao, M. McDowell, I. Ryu, H. Wu, N. Liu, L. Hu, Y. Cui, Interconnected silicon hollow nanospheres for lithium-ion battery anodes with long cycle life, Nano Lett. 11 (2011) 2949–2954.
[37] H. Li, H. Zhou, Enhancing the performances of Li-ion batteries by carbon-coating: present and future, Chem. Commun. 48 (2012) 1201–1217.
[38] K. Karki, Y. Zhu, Y. Liu, C. Sun, L. Hu, Y. Wang, Hoop-strong nanotubes for battery electrodes, ACS Nano 7 (2013) 8295–8302.
[39] G. Sandu, L. Brassart, J. Gohy, T. Pardoen, S. Melinte, A. Vlad, Surface coating mediated swelling and fracture of silicon nanowires during lithiation, ACS Nano 8 (2014) 9427–9436.
[40] S. Sim, P. Oh, S. Park, J. Cho, Critical thickness of SiO_2 coating layer on core@shell bulk@nanowire Si anode materials for Li-ion batteries, Adv. Mater. 25 (2013) 4498–4503.
[41] H. Wu, G. Chan, J. Choi, I. Ryu, Y. Yao, M. McDowell, Y. Cui, Stable cycling of double-walled silicon nanotube battery anodes through solid-electrolyte interphase control, Nature Nanotechnol. 7 (2012) 309–314.
[42] X. Han, Y. Liu, Z. Jia, Y. Chen, J. Wan, N. Weadock, T. Li, L. Hu, Atomic-layer-deposition oxide nanoglue for sodium ion batteries, Nano Lett. 14 (2014) 139–147.
[43] T. Li, Z. Suo, S. Lacour, S. Wagner, Compliant thin film patterns of stiff materials as platforms for stretchable electronics, J. Mater. Res. 20 (2005) 3274–3277.
[44] S. Lacour, D. Chan, S. Wagner, T. Li, Z. Suo, Mechanisms of reversible stretchability of thin metal films on elastomeric substrates, Appl. Phys. Lett. 88 (2006).
[45] S. Lacour, J. Jones, S. Wagner, T. Li, Z. Suo, Stretchable interconnects for elastic electronic surfaces, Proc. IEEE 93 (2005) 1459–1467.
[46] S. Wagner, S. Lacour, J. Jones, P. Hsu, J. Sturm, T. Li, Z. Suo, Electronic skin: architecture and components, Phys. E-Low-Dimens. Syst. Nanostructures 25 (2004) 326–334.
[47] D. Kim, N. Lu, R. Ma, Y. Kim, R. Kim, S. Wang, J. Rogers, Epidermal electronics, Science 333 (2011) 838–843.
[48] T. Bhandakkar, H. Johnson, Diffusion induced stresses in buckling battery electrodes, J. Mech. Phys. Solids 60 (2012) 1103–1121.
[49] M. Pharr, Z. Suo, J. Vlassak, Measurements of the fracture energy of lithiated silicon electrodes of Li-ion batteries, Nano Lett. 13 (2013) 5570–5577.
[50] J. Maranchi, A. Hepp, A. Evans, N. Nuhfer, P. Kumta, Interfacial properties of the a-Si/Cu: active–inactive thin-film anode system for lithium-ion batteries, J. Electrochem. Soc. 153 (2006) A1246–A1253.
[51] X. Chen, J. Hutchinson, Herringbone buckling patterns of compressed thin films on compliant substrates, J. Appl. Mech.-Trans. ASME 71 (2004) 597–603.
[52] J. Zang, X. Zhao, Y. Cao, J. Hutchinson, Localized ridge wrinkling of stiff films on compliant substrates, J. Mech. Phys. Solids 60 (2012) 1265–1279.
[53] X. Liu, H. Zheng, L. Zhong, S. Huan, K. Karki, L. Zhang, J. Cummings, J. Huang, Anisotropic swelling and fracture of silicon nanowires during lithiation, Nano Lett. 11 (2011) 3312–3318.
[54] M. Mortazavi, J. Deng, V. Shenoy, N. Medhekar, Elastic softening of alloy negative electrodes for Na-ion batteries, J. Power Sources 225 (2013) 207–214.
[55] T. Li, Z. Huang, Z. Suo, S. Lacour, S. Wagner, Stretchability of thin metal films on elastomer substrates, Appl. Phys. Lett. 85 (2004) 3435–3437.
[56] T. Li, Z. Huang, Z. Xi, S. Lacour, S. Wagner, Z. Suo, Delocalizing strain in a thin metal film on a polymer substrate, Mech. Mater. 37 (2005) 261–273.
[57] T. Li, Z. Suo, Deformability of thin metal films on elastomer substrates, Internat. J. Solids Structures 43 (2006) 2351–2363.
[58] M. Pharr, K. Zhao, X. Wang, Z. Suo, J. Vlassak, Kinetics of initial lithiation of crystalline silicon electrodes of lithium-ion batteries, Nano Lett. 12 (2012) 5039.
[59] Z. Jia, T. Li, Intrinsic stress mitigation via elastic softening during two-step electrochemical lithiation of amorphous silicon, submitted for publication, 2015.
[60] Z. Jia, C. Peng, J. Lou, T. Li, A map of competing buckling-driven failure modes of substrate-supported thin brittle films, Thin Solid Films 520 (2012) 6576.

Please cite this article in press as: Z. Jia, T. Li, Failure mechanics of a wrinkling thin film anode on a substrate under cyclic charging and discharging, Extreme Mechanics Letters (2016), http://dx.doi.org/10.1016/j.eml.2016.03.006